Absolute versus convective instability of spiral waves

Björn Sandstede
Department of Mathematics, Ohio State University, 231 West 18th Avenue, Columbus, Ohio 43210

Arnd Scheel
Institut für Mathematik I, Freie Universität Berlin, Arnimallee 2-6, 14195 Berlin, Germany
(Received 26 May 2000)

Absolute and convective instabilities of spirals are investigated using the continuous and the so-called absolute spectrum. It is shown that the nature of transport, induced by an absolute instability, is determined by spectral data of the asymptotic wave trains. The results are applied to core and far-field breakup of spiral waves in excitable and oscillatory media.

PACS number(s): 82.40.Ck, 47.54.+r, 05.45.−a

I. INTRODUCTION

Spiral waves have been observed in various biological, chemical, and physical systems [1], for instance, in the Belousov-Zhabotinsky reaction, during fibrillations in cardiac tissue, and in the oxidation of carbon-monoxide on platinum surfaces. They have also been found in numerical simulations of reaction-diffusion systems and complex Ginzburg-Landau equations on planar domains. Spiral waves can destabilize in many different ways. For instance, they may begin to meander or to drift, a scenario that has been attributed to a Hopf instability [2]. Alternatively, transverse instabilities may occur [3] that are characterized by a degenerate dispersion relation between asymptotic wavelength and wave speed. Another common instability is the breakup of spiral waves, which comes in two ''flavors'': either the core [4] or the far field [5,6] of the spiral breaks up into a turbulent region with complex spatiotemporal behavior. Far-field breakup of spiral waves was observed in experiments [5].

In this paper, we concentrate on a linear stability analysis of spiral waves to link spectral properties of spirals to the direction of transport that they induce: Suppose that we add a small localized humplike perturbation to the spiral wave, and monitor the time evolution of the corresponding solution. If the spiral wave is unstable, the localized perturbation will certainly grow: We say that the spiral transports toward the core if the center of mass of the perturbation, i.e., the position of its peak, moves toward the core. If the center of mass of the perturbation moves away from the core toward the boundary of the domain, we say that the spiral transports toward the boundary. This notion of transport is made more precise below by using exponential weights. To relate spectral properties of the spiral waves and the direction of transport, we investigate the spectra of spiral waves on the plane and on large bounded disks. First, for spiral waves on the plane, we demonstrate that the continuous spectrum of the spiral can be computed from the spectrum of the asymptotic wave trains, but that the two spectra differ by translations along the imaginary axis. The group velocities of spirals and wave trains, computed in the laboratory frame, are the same. Next we consider spiral waves on large but bounded disks. On a linear level, the temporal evolution of localized perturbations is then determined by the eigenmodes that are associated with the continuous spectrum, at least as long as the localized perturbation stays away from the boundary; indeed, the localized perturbation is then not affected by the boundary conditions, and it therefore behaves in the same way as on the entire plane. Alternatively, the temporal behavior of localized perturbations can be described in terms of the absolute spectrum, introduced in Ref. [12], which is related to the spectrum of the spiral wave on large disks. This latter description is also valid if the localized perturbation approaches the boundary of the domain. The rightmost point of the absolute spectrum is typically given by a double root of the linear dispersion relation. We characterize the entire absolute spectrum, and not only its rightmost point, and investigate the spatial shape of eigenfunctions in the absolute spectrum using exponential weights that break the translation symmetry of the plane. As a consequence, the direction of transport, induced by absolute instabilities, can be predicted from spectral data of the asymptotic wave trains. Our analytical results also provide means of computing continuous and absolute spectra easily from the asymptotic wave trains using boundary-value problem solvers such as AUTO97 [7]. We emphasize that our approach is based on a linear stability analysis; a sensitive nonlinearity may result in a quite different behavior.

Part of our motivation comes from attempting to understand the nature of spiral-wave breakup in excitable and oscillatory media. It appears from our numerical simulations that the difference between core and far-field breakup cannot be explained solely by the direction of transport induced by absolute instabilities. Instead the group velocities of the continuous spectrum seem to play an important role.

A second consequence of the approach adopted here is that it allows us to predict the superstructures of meandering and drifting spiral waves. The shape of the superstructures is closely related to eigenmodes in the continuous spectrum. This issue was explored in Ref. [8].

Consider a reaction-diffusion model

$$u_t = D\Delta u + f(u), \quad u \in \mathbb{R}^m, \quad x \in \mathbb{R}^2 \tag{1}$$

on the plane. Archimedean spiral waves are solutions to Eq. (1) that rotate rigidly with a constant angular velocity c, and

that are asymptotically periodic along rays in the plane. In a corotating coordinate frame, Eq. (1) is given by

$$u_t = D\Delta u + cu_\varphi + f(u), \quad x \in \mathbb{R}^2,$$

where (r,φ) denote polar coordinates. A spiral wave is then a stationary solution given by $u_*(r,\varphi)$ with $u_*(r,\varphi) \to u_\infty(\kappa r+\varphi)$ as $r\to\infty$ for some 2π-periodic function $u_\infty(\psi)$. The function $u_\infty(\psi)$ is a stationary wave-train solution to

$$u_t = D\kappa^2 u_{\psi\psi} + cu_\psi + f(u), \quad \psi \in \mathbb{R}. \tag{2}$$

The asymptotic wave number κ and the wave speed c are related via a nonlinear dispersion relation.

II. SPECTRA OF ASYMPTOTIC WAVE TRAINS

We begin by analyzing the spectrum of the asymptotic wave trains $u_\infty(\psi)$ to Eq. (2). The eigenvalue problem is given by

$$D\kappa^2 v_{\psi\psi} + cv_\psi + f'(u_\infty(\psi))v = \tilde{\lambda} v, \quad \psi \in \mathbb{R}. \tag{3}$$

It follows from Floquet theory that $\tilde{\lambda} \in \mathbb{C}$ is an eigenvalue of the wave train if, and only if, the system

$$\begin{aligned} &D\kappa^2 v_{\psi\psi} + cv_\psi + f'(u_\infty(\psi))v = \tilde{\lambda} v, \quad 0<\psi<2\pi, \\ &(v,v_\psi)(2\pi) = e^{2\pi i\tilde{\gamma}}(v,v_\psi)(0) \end{aligned} \tag{4}$$

has a solution v for some $\tilde{\gamma} \in \mathbb{R}$. Eigenvalues come in curves $\tilde{\lambda} = \tilde{\lambda}(i\tilde{\gamma})$; note that one of these curves contains $\tilde{\lambda}=0$, with $\tilde{\gamma}=0$ and $v(\psi)=u_\infty'(\psi)$.

Upon varying parameters, the wave train might destabilize in an Eckhaus instability. Eckhaus instabilities are either of convective nature or are absolute instabilities. The difference between these two kinds of instability is that, for a convective instability, perturbations grow but are also convected away; in other words, the perturbation actually decays locally, at least eventually for large values of time, at every fixed point in the domain, while the position of the growing maxima of the perturbation travels toward infinity. In contrast, for absolute instabilities, perturbations grow everywhere, i.e., at every given point in the domain. Previously, absolute instabilities have been located by seeking certain double roots of the linear dispersion relation $\tilde{\lambda}(\tilde{\nu})$ of Eq. (3) that relates spatial wavenumbers $\tilde{\nu} \in \mathbb{C}$ to temporal decay or growth rates $\tilde{\lambda} \in \mathbb{C}$; see Refs. [9,10]. Here we propose a different way of computing absolute instabilities that, in addition, gives more information about their nature. The idea, which goes back to Ref. [11], is to use exponential weights $\exp(-\tilde{a}\psi)$ to measure transport. Thus we solve the linearized equation

$$v_t = D\kappa^2 v_{\psi\psi} + cv_\psi + f'(u_\infty(\psi))v,$$

and monitor $\|\exp(-\tilde{a}\psi)v(t,\psi)\|$ instead of $\|v(t,\psi)\|$ as $t\to\infty$. For $\tilde{a}>0$, this allows solutions to grow exponentially with rate up to $\tilde{a}$ as $\psi\to\infty$; in other words, it stabilizes eigenmodes that correspond to transport toward $+\infty$. Similarly, $\tilde{a}<0$ stabilizes eigenmodes that correspond to transport toward $-\infty$. We shall compute the spectrum using the exponential weight $\exp(-\tilde{a}\psi)$. It follows that $\tilde{\lambda}$ is in the spectrum of the wave train, computed with weight $\exp(-\tilde{a}\psi)$, if there is a solution $v(\psi)$ to Eq. (3) such that $\exp(-\tilde{a}\psi)v(\psi)$ is bounded, but does not decay. Hence we see that $\tilde{\lambda}$ is in the continuous spectrum, computed with the weight $\exp(-\tilde{a}\psi)$, if and only if

$$\begin{aligned} &D\kappa^2 v_{\psi\psi} + cv_\psi + f'(u_\infty(\psi))v = \tilde{\lambda} v, \quad 0<\psi<2\pi, \\ &(v,v_\psi)(2\pi) = e^{2\pi(\tilde{a}+i\tilde{\gamma})}(v,v_\psi)(0), \end{aligned} \tag{5}$$

has a solution v for some $\tilde{\gamma} \in \mathbb{R}$. The curves $\tilde{\lambda}(\tilde{a}+i\tilde{\gamma})$, computed for fixed $\tilde{a}$, are typically shifted with respect to the spectrum $\tilde{\lambda}(i\tilde{\gamma})$ that we computed without weights. If the weighted spectrum is shifted to the left in the complex plane, then the sign of the corresponding value of $\tilde{a}$ determines whether transport occurs to the right $(\tilde{a}>0)$ or to the left $(\tilde{a}<0)$. We emphasize that the criterion [9,10] that uses double roots of the linear dispersion relation $\tilde{\lambda}(\tilde{a}+i\tilde{\gamma})$ is different from our criterion that employs exponential weights; for instance, if counterpropagating eigenmodes are present, so that transport occurs simultaneously toward $+\infty$ and $-\infty$, then exponential weights destabilize [12], while the criterion [9,10] still stabilizes.

Both systems (4) and (5) can be solved numerically using a continuation code for boundary-value problems such as AUTO97 (see Ref. [7] for this package). A starting solution is given by $\tilde{\lambda}=0$, $\tilde{\gamma}=0$ and $v(\psi)=u_\infty'(\psi)$; afterward, this solution is continued in the wave number $\tilde{\gamma}$. The advantage of this approach is that it gives the continuous spectrum in terms of curves $\tilde{\lambda}(i\tilde{\gamma})$ that are parameterized by the wave number $\tilde{\gamma}$.

III. CONTINUOUS SPECTRA OF PLANAR SPIRAL WAVES

In the next step, we consider the spectrum of the spiral wave $u_*(r,\varphi)$. The eigenvalue problem for planar spiral waves reads

$$D\Delta_{r,\varphi} v + cv_\varphi + f'(u_*(r,\varphi))v = \lambda v. \tag{6}$$

We shall ignore isolated eigenvalues that belong to the point spectrum; instabilities caused by point eigenvalues lead to meandering or drifting waves in excitable media [2], or to an unstable tip motion in oscillatory media [13]. Instead, we focus on the continuous spectrum that is responsible for spiral-wave breakup. Using the results in Ref. [14], it turns out that the boundary of the continuous spectrum depends only on the limiting equation for $r\to\infty$. Using $\Delta_{r,\varphi} = \partial_{rr} + r^{-1}\partial_r + r^{-2}\partial_{\varphi\varphi}$, we have that λ is in the boundary of the continuous spectrum if, and only if,

$$Dv_{rr} + cv_\varphi + f'(u_\infty(\kappa r+\varphi))v = \lambda v$$

has a solution $v(r,\varphi)$ for $(r,\varphi) \in \mathbb{R}^+ \times [0,2\pi]$ that is bounded but does not decay as $r\to\infty$. Transforming $(r,\varphi) \to (r,\psi) = (r,\kappa r+\varphi)$, we seek bounded solutions to

$$D(\partial_r + \kappa\partial_\psi)^2 v + cv_\psi + f'(u_\infty(\psi))v = \lambda v.$$

Using Fourier transform, we see that any bounded solution is of the form $v(r,\psi)=\exp(i\gamma r)w(\psi)$ for some $\gamma\in\mathbb{R}$, where $w(\psi)$ is 2π periodic in ψ. Writing $w(\psi)=\exp(-i\gamma\psi/\kappa)V(\psi)$, we conclude that λ is in the boundary of the continuous spectrum if, and only if, $V(\psi)$ satisfies

$$D\kappa^2V_{\psi\psi}+cV_\psi+f'(\mathbf{u}_\infty(\psi))V=\left(\lambda+\frac{i\gamma c}{\kappa}\right)V,$$
$$(V,V_\psi)(2\pi)=e^{2\pi i\gamma/\kappa}(V,V_\psi)(0) \tag{7}$$

for some $\gamma\in\mathbb{R}$, where $0<\psi<2\pi$. We are now in a position to compare the boundary of the continuous spectrum of the planar spiral wave $u_*(r,\varphi)$ with the continuous spectrum of the associated asymptotic wave train $u_\infty(\psi)$. Comparing Eqs. (4) and (7), we see that the boundary of the continuous spectrum of the spiral wave is parametrized by

$$\lambda=\tilde\lambda(i\tilde\gamma)-ic(\tilde\gamma+l),\quad \gamma=\kappa(\tilde\gamma+l), \tag{8}$$

where $l\in\mathbb{Z}$ is arbitrary, and $\tilde\lambda(i\tilde\gamma)$ denotes the spectrum of the wave train computed according to Eq. (4). Note that the spectra of the spiral wave and the asymptotic wave train are not quite the same, even though their maximal real parts coincide, so that the spiral wave destabilizes at the same moment as the associated wave train. We shall see below where the additional term in Eq. (8) comes from.

IV. CONVECTIVE SPECTRA OF PLANAR SPIRAL WAVES

The continuous spectrum computed above gives information about the stability versus instability of the spiral wave considered on the unbounded plane. In the next step, we explore whether small perturbations that are added to the spiral wave are convected toward or away from the core. This information cannot be gleaned from the location of the spectrum in Eq. (8) alone, since convection is not related to overall decay or growth as measured by the continuous spectrum but to local decay or growth. As before, we compute the spectrum using exponential weights that penalize perturbations that are convected in the radial direction. Hence we shall solve

$$v_t=D\Delta_{r,\varphi}v+cv_\varphi+f'(u_*(r,\varphi))v,$$

and monitor $\|\exp(-ar)v(t,r,\varphi)\|$ as $t\to\infty$. For $a>0$, this allows solutions to grow exponentially as $r\to\infty$; in other words, eigenmodes that correspond to transport away from the core are stabilized. Similarly, $a<0$ stabilizes eigenmodes that correspond to transport toward the core. Our result states that λ is in the spectrum of the planar spiral wave, computed with weight $\exp(-ar)$, if there is a solution $v(r,\varphi)$ to Eq. (6) such that $\exp(-ar)v(r,\varphi)$ is bounded. Arguing as above, we see that λ is in the boundary of the continuous spectrum of the spiral wave, computed with weight $\exp(-ar)$ if, and only if,

$$D\kappa^2V_{\psi\psi}+cV_\psi+f'(u_\infty(\psi))V=\left(\lambda+\frac{c}{\kappa}(a+i\gamma)\right)V,$$
$$(V,V_\psi)(2\pi)=e^{2\pi(a+i\gamma)/\kappa}(V,V_\psi)(0) \tag{9}$$

has a solution $V(\psi)$ for some $\gamma\in\mathbb{R}$, where $0<\psi<2\pi$. The associated eigenmode of Eq. (6) is then of the form

$$e^{-(a+i\gamma)\varphi/\kappa}V(\kappa r+\varphi)$$

as $r\to\infty$; note that this eigenmode grows, or decays, exponentially with rate a as $r\to\infty$.

It remains to show that the spectrum of the spiral wave, computed with weight $\exp(-ar)$, can also be calculated using the asymptotic wave trains. Upon inspecting Eqs. (5) and (9), it follows that the boundary of the weighted spectrum of the spiral wave is given by

$$\lambda=\tilde\lambda\left(\frac{a}{\kappa}+i\tilde\gamma\right)-\frac{ac}{\kappa}-ic(\tilde\gamma+l),$$

where $l\in\mathbb{Z}$ is arbitrary, and $\tilde\lambda(a/\kappa+i\tilde\gamma)$ denotes the weighted spectrum of the wave train computed according to Eq. (5) with $\tilde a=a/\kappa$. The factor c/κ is positive whenever the wave is spiraling outwardly; thus, for outwardly spiraling waves, the term ac/κ stabilizes the wave for $a>0$ which corresponds to transport away from the core. This additional transport is created by compensating for the moving frame in which we computed the weighted spectrum of the asymptotic wave train; indeed, in Eq. (5), we imposed the weight $\exp(-\tilde a\psi)$ on perturbations in a frame that moves with speed c. To compensate for the moving frame, we should compute the weighted spectrum of the wave trains using the time-dependent weight $\exp(-\tilde a(\psi+ct))$ that corresponds to the exponential weight $\exp(-\tilde a\phi)$ in the laboratory frame $\phi=\psi+ct$. The effect on the weighted spectrum is that $\tilde\lambda$ is replaced by $\tilde\lambda-\tilde ac$, i.e., by $\tilde\lambda-ac/\kappa$. In addition, this analysis establishes that the behavior of one-dimensional wave trains that are generated by Dirichlet sources precisely captures the convective behavior of spiral waves (provided the wavelength selected by the Dirichlet source is the same as that selected by the spiral wave—this, however, is typically not the case). Hence, our analysis corroborates the conclusions in Ref. [6], where direct numerical simulations of such wave trains were used.

In summary, localized perturbations added to the spiral in its far field can be transported toward the core or toward the boundary of the domain. These two cases can be distinguished, at least on a linear level, by computing the spectrum of the asymptotic wave trains using appropriate exponential weights: If certain unstable modes stabilize for positive rates $a>0$, then the spiral transports toward the boundary. If the modes stabilize with a negative weight $a<0$, localized perturbations added to spiral waves are transported toward the core. At the onset of instability, stability properties depend on the derivative $-d\,\mathrm{Re}\,\lambda/da=-d\,\mathrm{Im}\,\lambda/d\gamma$, which is the group velocity of the asymptotic wave trains, computed in the laboratory frame.

Before we address the relevance of our results for spirals on large but bounded disks, we report on transport of (marginally) stable spiral waves on the entire plane. Suppose that the asymptotic wave trains are marginally stable, so that the curve $\tilde\lambda(i\tilde\gamma)$ that contains $\lambda=0$ is of the form $\tilde\lambda(i\tilde\gamma)=id_1\tilde\gamma-d_2\tilde\gamma^2$ for some $d_2>0$, and so that all remaining spectral curves are strictly to the left of the imaginary axis. Assume, furthermore, that the nonlinear dispersion relation

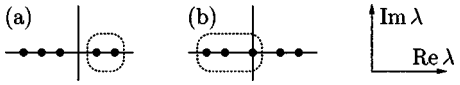

FIG. 1. The spatial spectra of Eq. (10), linearized about the core state (a) and the wave train (b), are plotted. The dimensions of the unstable manifold of the core state and the center-stable manifold of the wave train have to add up to the phase-space dimension.

which relates the asymptotic wavelength κ to the angular velocity c of the spiral is nondegenerate. It is then true that the spiral wave automatically transports away from the core, i.e., the spiral is stable in the weight $\exp(-ar)$ for any $a>0$ sufficiently small, so that the weighted continuous spectrum is strictly to the left of the imaginary axis. We argue as follows. We seek spiral waves as stationary patterns to $D\Delta u+cu_\varphi+f(u)=0$, and cast this equation as a first-order initial-value problem in the radial variable r:

$$\begin{aligned} u_r&=v,\\ v_r&=-\left[\frac{v}{r}+\frac{u_{\varphi\varphi}}{r^2}+D^{-1}[cu_\varphi+f(u)]\right]. \end{aligned} \tag{10}$$

Spiral waves $u_*(r,\varphi)$ can then be thought of as fronts in the radial variable r that connect the core state $u_*(0,\varphi)$ at $r=0$ with the r-periodic wave train $u_\infty(\kappa r+\varphi)$ as $r\to\infty$. In other words, spirals are solutions to Eq. (10) that are contained in the intersection of the unstable manifold, with respect to Eq. (10) with r as the evolution variable, of the core state $u_*(0,\varphi)$ and the center-stable manifold of the wave train $u_\infty(\kappa r+\varphi)$; note that the linearization of Eq. (10) about the wave train has a bounded solution, namely, $u'_\infty(\kappa r+\varphi)$. It turns out that both invariant manifolds are infinite dimensional, and we cannot easily count dimensions, or codimensions, and apply transversality arguments. For the sake of clarity, we pretend that these dimensions are both finite, and refer to Ref. [14] for the more correct argument where dimensions are counted by means of a comparison to a reference equation. Since we assumed that the nonlinear dispersion relation is nondegenerate, the spiral wave is locally unique; therefore, the dimensions of the unstable manifold of the core state and the center-stable manifold of the wave train have to add up to the dimension of the phase space, so that the spectra of the linearization of Eq. (10) about the core state and the wave train are as shown in Fig. 1.

Next, we apply the same arguments to the linearization [Eq. (6)]

$$\begin{aligned} u_r&=v,\\ v_r&=-\left[\frac{v}{r}+\frac{u_{\varphi\varphi}}{r^2}+D^{-1}\{cu_\varphi+[f'(u_*(r,\varphi))-\lambda]u\}\right] \end{aligned} \tag{11}$$

about the spiral wave, again written as a first-order system in r. For $\lambda=0$, Eq. (11) and the linearization of Eq. (10) about the spiral coincide; furthermore, as discussed above, the dimensions of the unstable eigenspace of Eq. (11) at the core state and those of the center-stable eigenspace of Eq. (11) at the asymptotic wave train add up to the dimension of the phase space. For $\lambda>0$, the eigenvalue $\nu=0$ of the asymptotic wave train moves either to the left [see Fig. 2(b)] or the right [see Fig. 2(c)] of the imaginary axis. Since we assumed that $\mathrm{Re}\,\lambda>0$ does not contain any points in the spectrum of the wave train, and therefore no points in the spectrum of the spiral wave, the aforementioned dimensions still add up to the dimension of the phase space [12]. Hence, only the case shown in Fig. 2(b) can occur, so that $\lambda(a)>0$ for $a<0$, where $\nu=a$ is the perturbed spatial eigenvalue near $\nu=0$; in particular, we have $d\lambda/d\nu<0$ at $\nu=0$ which means that the group velocity $c_{\mathrm{gr}}=-d\,\mathrm{Im}\,\lambda/d\gamma>0$ is always positive at $\nu=0$. As a consequence, $\lambda(a)<0$ for $a>0$, which proves that the spiral-wave spectrum moves into the left half-plane when we compute it with a weight $\exp(-ar)$ for sufficiently small $a>0$. As a consequence, marginally stable spiral waves always transport away from the core: the group velocity of the emitted wave trains is always positive.

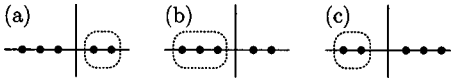

FIG. 2. The spatial spectrum of Eq. (11) about the core state is plotted in (a). In (b) and (c), the spatial spectrum of Eq. (11) about the asymptotic wave train is plotted for $\lambda>0$; the eigenvalue $\nu=0$ of Eq. (11) at $\lambda=0$ could move either to the left (b) or the right (c). The coordinates are as in Fig. 1.

V. ABSOLUTE SPECTRA OF SPIRAL WAVES ON LARGE BUT BOUNDED DISKS

Finally, we discuss the spectra of spiral waves when the domain is not the plane but a large bounded disk. This issue was addressed previously in Refs. [9,15–17] for the complex Ginzburg-Landau equation. In these references, it was observed that only absolute instabilities on the plane persist as instabilities on large bounded domains, independently of the size of the domain. Note that the spectrum of the spiral on a disk of radius R consists entirely of point spectrum. Introduced in Ref. [12], the absolute spectrum of the spiral is defined as the limit, as the radius $R\to\infty$ tends to infinity, of the spectra on disks of radius R. Each point in the absolute spectrum is approached, as $R\to\infty$, by infinitely many different eigenvalues of the spiral on the disk of radius R. Thus the absolute spectrum gives the asymptotic position of the eigenvalues on large disks. We showed in Ref. [12] how the absolute spectrum can be computed analytically for any reaction-diffusion system: Consider the eigenvalue problem for the asymptotic wave train,

$$\begin{aligned} u_r&=v,\\ v_r&=-\left[\frac{v}{r}+\frac{u_{\varphi\varphi}}{r^2}+D^{-1}(cu_\varphi+\{f'[u_\infty(\kappa r+\varphi)]-\lambda\}u)\right] \end{aligned} \tag{12}$$

written as a first-order system in the radial variable r. For a given $\lambda\in\mathbb{C}$, we compute the spatial eigenvalues $a+i\gamma$ where a corresponds to the spatial decay or growth rate of solutions to Eq. (12), and γ to their spatial wave number. For each λ, there are infinitely many stable and unstable spatial eigenvalues. We plot λ in the complex plane, and attach to each λ the associated spatial spectrum; see Fig. 3. Thus λ is in the continuous spectrum of the planar spiral wave if the

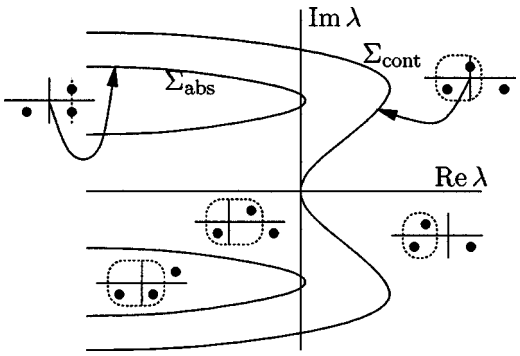

FIG. 3. The spectra Σ_{cont} and Σ_{abs} of the spiral wave on the entire plane and large bounded disks are plotted; the insets show the spatial eigenvalues $\nu=a+i\gamma$ of Eq. (12) computed for fixed λ in the aforementioned spectra, and in the regions between these spectra.

associated spatial spectrum has points on the imaginary axis. The absolute spectrum is determined as follows. For large $\lambda>0$, we consider the stable and unstable eigenspaces of Eq. (12); both spaces are infinite dimensional (see above), but we pretend as before that they both have finite dimension. We vary $\lambda\in\mathbb{C}$, and plot the spatial eigenvalues. We showed in Ref. [12] that λ is in the absolute spectrum if there are formerly stable and formerly unstable spatial eigenvalues that now have the same real part; see Fig. 3. If this real part is positive, then the associated eigenmodes grow exponentially toward the boundary, i.e., they correspond to a far-field instability; if the real part is negative, then the eigenmodes grow toward the core, and the instability occurs near the core. Often, the edge of the absolute spectrum corresponds to a point where formerly stable and formerly unstable spatial eigenvalues coalesce—this occurs at double roots of the linear dispersion relation, as predicted in Ref. [9]. The resulting linear eigenmode has zero group velocity, while the eigenmodes obtained for spatial eigenvalues with the same real part but a different imaginary part have nonzero group velocity. The condition that one of the two colliding spatial eigenvalues is stable while the other one is unstable for large positive λ is often referred to as the pinching condition [18]. We emphasize that the aforementioned characterization of the rightmost point of the absolute spectrum as a double root of the linear dispersion relation is only true if the most unstable eigenmode has a zero group velocity. If the linearized equation sustains counterpropagating waves, the most unstable mode can have a nonzero group velocity; we refer to Ref. [12] for examples. As a consequence, it might be necessary to compute the entire absolute spectrum as outlined above to determine the onset to instability.

VI. ONSET TO INSTABILITY ON BOUNDED DOMAINS

In summary, we have demonstrated that it is possible to predict the location and nature of an absolute instability, i.e., whether it causes breakup near the core or in the far field, on the entire plane as well as on any large bounded domain, by investigating only the eigenvalue problem of the asymptotic wave train upon using appropriate exponential weights. We shall argue, however, that the transition to instability on bounded domains does not occur at a well defined point in parameter space; instead, spiral waves typically destabilize somewhere in between the convective and the absolute Eckhaus instability. Indeed, in the region between these two instabilities, we can always stabilize spiral waves on bounded domains by using exponential weights $\exp(-ar)$, with $a>0$ for a core and $a<0$ for a far-field convective instability. Thus the fate of an initial condition that is close to the spiral wave depends upon the time evolution computed with the exponential weight. In particular, for stability, the initial condition has to be sufficiently close to the spiral wave, again with respect to the exponential weight, due to the nonlinear terms [12]. As a consequence, if the Eckhaus instability corresponds to transport toward the boundary, and if the radius of the bounded domain is R, then only those initial conditions that are $\exp(-aR)$ close to the spiral wave near the core will ultimately converge toward the spiral—any other initial condition is amplified well before the perturbation disappears through the boundary; this will lead to spiral-wave breakup near the boundary. Analogously, if the Eckhaus instability corresponds to transport toward the core, then only those initial conditions that are $\exp(aR)$ close, with $a<0$, to the spiral wave near the boundary will ultimately converge toward the spiral; any other initial condition is amplified so much that the spiral breaks up near the core.

VII. CORE VERSUS FAR-FIELD BREAKUP

We apply the results obtained above to the system

$$u_t=\Delta u-\frac{1}{\epsilon}u(u-1)\left(u-\frac{b+v}{a}\right),$$

$$v_t=f(u)-v, \tag{13}$$

$$f(u)=\begin{cases}0, & 0\leqslant u<1/3\\ 1-6.75u(u-1)^2, & 1/3\leqslant u\leqslant 1\\ 1, & 1<u\end{cases}$$

that has been used to model patterns in catalytic surface reactions [4,6]. We are interested in the following two parameter regimes:

$$\text{excitable:}\quad a=0.75,\quad b=6\times 10^{-4}, \tag{14}$$

$$\text{oscillatory:}\quad a=0.84,\quad b=-0.045. \tag{15}$$

The second parameter regime [Eq. (15)] was investigated earlier [6]. Direct numerical simulations using Barkley's code EZSPIRAL show that the spiral wave exhibits a core breakup for parameters as in Eq. (14) with $\epsilon=0.072$, while we observed a far-field breakup for parameter values [Eq. (15)] with $\epsilon=0.075$; see Fig. 4. To investigate the nature of transport and the difference between core and far-field breakup, we first computed the onset to absolute and convective (Eckhaus) instability of the spiral waves using AUTO97, and compared these predictions with direct simulations. The results are shown in Fig. 5. They confirm that it is indeed the absolute spectrum, and not the continuous spectrum, that is relevant for instabilities on bounded domains.

Next, we computed the absolute and the continuous spectrum of the spiral waves at the point in parameter space

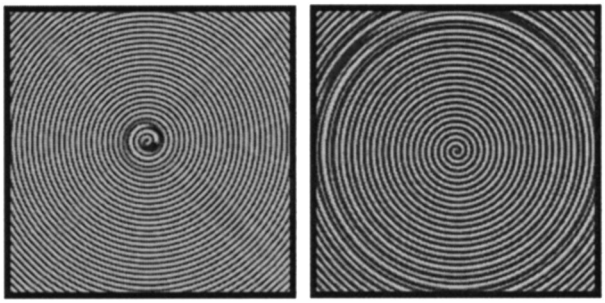

FIG. 4. Spiral waves to Eq. (13) that exhibit a core breakup in the left plot [for parameter values of Eq. (14) with $\epsilon = 0.0724$] and a far-field breakup in the right plot [for parameter values of Eq. (15) with $\epsilon = 0.0746$].

where breakup occurs. The results are shown in Fig. 6. The spectra at core and far-field breakup look quite similar. To determine the nature of transport, we plotted the real part of λ for λ in the absolute spectrum versus the exponential growth rate a per wave-train period. The results are shown in the upper plot in Fig. 7. Note that the rate is positive for both core and far-field breakup. We conclude that, even in the case of a core breakup, transport eventually occurs toward the boundary. In the lower plot in Fig. 7, the group velocity of eigenmodes in the continuous spectrum is shown as a function of the real part of λ where λ varies in the continuous spectrum. Thus it appears as if the eigenmodes in the absolute spectrum still correspond to transport toward the boundary, even near core breakup. There is, however, a quantitative difference between the eigenmodes near core and far-field breakup. The results presented in Fig. 7 show that the exponential growth rate a, measured per wave-train period, is much smaller at core breakup than at far-field breakup. Thus the transport toward the boundary is far less pronounced. In addition, the group velocity is much smaller near core breakup compared with far-field breakup. In particular, the interval in Re λ over which the group velocity is

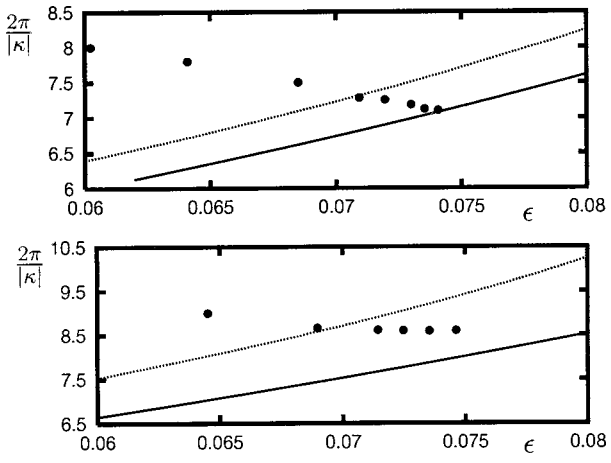

FIG. 5. The curves indicate the onset to absolute (solid lines) and Eckhaus instability (dotted lines) of spiral waves in the excitable regime [Eq. (14)] in the upper plot and in the oscillatory regime [Eq. (15)] in the lower plot. The vertical axis is the spatial period $2\pi/|\kappa|$ of the asymptotic wave trains, and the horizontal axis is ϵ. The circles indicate the results of direct simulations of Eq. (13) corresponding to the presence of spiral waves before breakup.

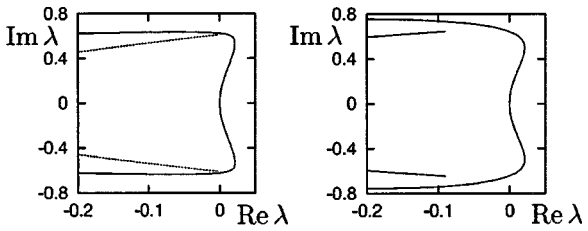

FIG. 6. The absolute spectra (dotted lines) and continuous spectra (solid lines) of spiral waves near the core breakup (left plot) and far-field breakup (BU) (right plot). We used asymptotic wave trains with a spatial period 7.1 and $\epsilon = 0.0741$ for core BU, and with a spatial period 8.6 and $\epsilon = 0.075$ for far-field BU: see Fig. 5.

negative (and therefore directed toward the core) is longer at core breakup.

Thus the difference between the core and far-field breakup could be related to the fact that, for core breakup, some of the eigenmodes belonging to the continuous spectrum transport localized perturbations toward the core over a broad interval of frequencies with a relatively small temporal decay, while the absolute eigenmodes are not yet visible owing to their slow exponential growth toward the boundary. At a far-field breakup, transport toward the boundaries is more prominent, since the absolute eigenmodes are growing much faster and the group velocity of the continuous eigenmodes is not as negative as for core breakup. In other words, the temporal evolution of a localized perturbation which is not close to the boundary can be described by both the entire set of absolute eigenmodes and the set of continuous eigenmodes. If some of the continuous eigenmodes transport fast enough toward the core, then the spiral can break up near the core, and the absolute eigenmodes that grow toward the boundary are not relevant.

VIII. CONCLUSIONS

We have investigated the structure of the spectrum of spiral waves by analytical means. In particular, we derived a

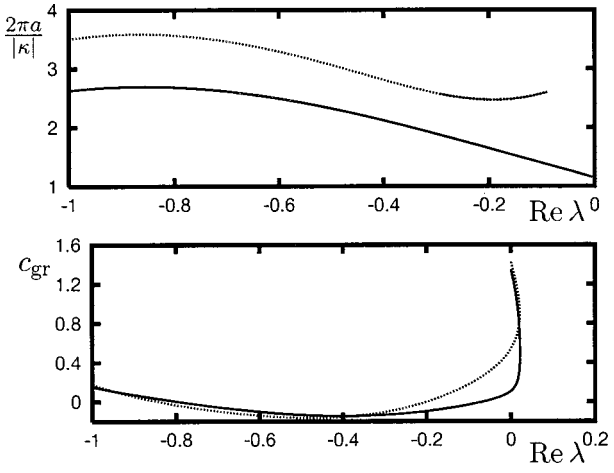

FIG. 7. The upper plot shows the exponential rate $2\pi a/|\kappa|$ per wave-train period as a function of Re λ for λ in the absolute spectrum of the spiral wave at core (solid line) and far-field (dotted line) breakups. The lower plot shows the group velocity $c_{gr} = -d\,\mathrm{Im}\,\lambda/d\gamma$ as a function of Re λ for λ in the continuous spectrum of the spiral wave at core (solid line) and far-field (dotted line) breakups. The parameter values used for both plots are as in Fig. 6.

characterization of the absolute spectrum of spirals on large disks in terms of the spatial spectra associated with the asymptotic wave trains. Furthermore, we related the continuous spectrum of spirals on the plane to the continuous spectrum of the asymptotic wave trains. We also confirmed that it is the absolute, and not the continuous, spectrum that causes instabilities on bounded disks; it should be emphasized, however, that the size of the allowed perturbation in the basis of attraction shrinks as the size of the disks increases. Absolute eigenmodes, however, are visible only after a transient regime that is governed by the continuous spectrum. It was demonstrated that the onset to absolute or convective instability, and in fact the absolute and continuous spectra themselves, can be computed numerically using formulation (5) as boundary-value problems together with a continuation code such as AUTO97. In addition, the use of exponential weights allowed us to predict the direction of transport at the onset to absolute or convective instabilities. Finally, we compared our predictions with numerical simulations of spiral waves that exhibit core and far-field breakup. It appears as if the absolute eigenmodes of spirals that break up near the core transport towards the boundary, at least on the level of a linear analysis, while at least some continuous eigenmodes transport toward the core. We believe that it is either this mechanism that causes core breakup or else the appearance of unstable point spectrum—note that such isolated eigenvalues have to cross the imaginary axis to the right of the continuous spectrum to cause core breakup [8]. Further analysis appears to be required to distinguish clearly between core and far-field breakup.

[1] A. T. Winfree, *When Time Breaks Down* (Princeton University Press, Princeton, 1987); *Chemical Waves and Patterns*, edited by R. Kapral and K. Showalter (Kluwer, Dordrecht, 1995); J. Murray, *Mathematical Biology* (Springer, Berlin, 1989); J. Keener and J. Sneyd, *Mathematical Physiology* (Springer, Berlin, 1998).
[2] D. Barkley, Phys. Rev. Lett. **68**, 2090 (1992); **72**, 164 (1994).
[3] A. Hagberg and E. Meron, Chaos **4**, 477 (1994).
[4] M. Bär and M. Eiswirth, Phys. Rev. E **48**, 1635 (1993).
[5] Q. Ouyang and J. M. Flesselles, Nature (London) **379**, 143 (1996).
[6] M. Bär and M. Or-Guil, Phys. Rev. Lett. **82**, 1160 (1999).
[7] E. J. Doedel, A. R. Champneys, T. F. Fairgrieve, Yu. A. Kuznetsov, B. Sandstede, and X. Wang (unpublished).
[8] B. Sandstede and A. Scheel (unpublished).
[9] I. S. Aranson, L. Aranson, L. Kramer, and A. Weber, Phys. Rev. A **46**, 2992 (1992).
[10] L. Brevdo and T. J. Bridges, Philos. Trans. R. Soc. London, Ser. A **354**, 1027 (1996).
[11] D. H. Sattinger, Adv. Math. **22**, 312 (1976).
[12] B. Sandstede and A. Scheel, Physica D **145**, 233 (2000).
[13] I. S. Aranson, L. Kramer, and A. Weber, Phys. Rev. Lett. **72**, 2316 (1994).
[14] B. Sandstede and A. Scheel, Math. Nachr. (to be published).
[15] H. Chaté and P. Manneville, Physica A **224**, 348 (1996).
[16] S. M. Tobias and E. Knobloch, Phys. Rev. Lett. **80**, 4811 (1998).
[17] S. M. Tobias, M. R. E. Proctor, and E. Knobloch, Physica D **113**, 43 (1998).
[18] R. J. Briggs, *Electron-Steam Interaction With Plasmas* (MIT Press, Cambridge, MA, 1964).